JACS
JOURNAL OF THE AMERICAN CHEMICAL SOCIETY
pubs.acs.org/JACS
Article

A Night-Time Edge Site Intermediate in the Cyanobacterial Circadian Clock Identified by EPR Spectroscopy

Gary K. Chow, Archana G. Chavan, Joel Heisler, Yong-Gang Chang, Ning Zhang, Andy LiWang,* and R. David Britt*

Cite This: J. Am. Chem. Soc. 2022, 144, 184−194
Read Online
ACCESS | Metrics & More | Article Recommendations | Supporting Information

ABSTRACT: As the only circadian oscillator that can be reconstituted *in vitro* with its constituent proteins KaiA, KaiB, and KaiC using ATP as an energy source, the cyanobacterial circadian oscillator serves as a model system for detailed mechanistic studies of day−night transitions of circadian clocks in general. The day-to-night transition occurs when KaiB forms a night-time complex with KaiC to sequester KaiA, the latter of which interacts with KaiC during the day to promote KaiC autophosphorylation. However, how KaiB forms the complex with KaiC remains poorly understood, despite the available structures of KaiB bound to hexameric KaiC. It has been postulated that KaiB-KaiC binding is regulated by inter-KaiB cooperativity. Here, using spin labeling continuous-wave electron paramagnetic resonance spectroscopy, we identified and quantified two subpopulations of KaiC-bound KaiB, corresponding to the "bulk" and "edge" KaiBC sites in stoichiometric and substoichiometric $KaiB_iC_6$ complexes (i = 1−5). We provide kinetic evidence to support the intermediacy of the "edge" KaiBC sites as bridges and nucleation sites between free KaiB and the "bulk" KaiBC sites. Furthermore, we show that the relative abundance of "edge" and "bulk" sites is dependent on both KaiC phosphostate and KaiA, supporting the notion of phosphorylation-state controlled inter-KaiB cooperativity. Finally, we demonstrate that the interconversion between the two subpopulations of KaiC-bound KaiB is intimately linked to the KaiC phosphorylation cycle. These findings enrich our mechanistic understanding of the cyanobacterial clock and demonstrate the utility of EPR in elucidating circadian clock mechanisms.

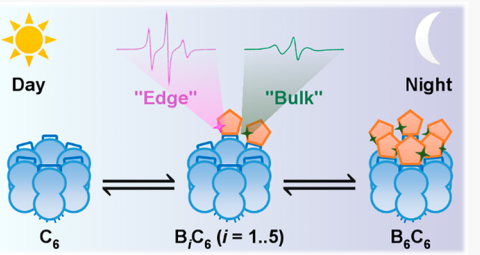

INTRODUCTION

Circadian clocks are endogenous biochemical oscillators that align diverse organisms' physiology with periodic day−night cycles,[1] thereby improving their survivability.[2] To study the molecular mechanisms governing circadian clocks, we turned to the cyanobacterial clock expressed by *Synechococcus elongatus* (PCC 7942) as its oscillator is entirely post-translational and can be reconstituted *in vitro*[3] in the absence of transcription or translation.[4] The circadian oscillator in *S. elongatus* consists of three proteins, KaiA, KaiB, and KaiC (Figure 1a), that when combined with ATP, generate a circadian rhythm in serine 431 (S431) and threonine 432 (T432) phosphorylations in KaiC via the cyclic sequence S;T → S;pT → pS;pT → pS;T → S;T → ... (p: phosphorylated)[5,6] (Figure 1a). During the day, KaiA acts as a nucleotide exchange factor of KaiC[7,8] by binding KaiC at the C-terminal loop region (A-loops)[9] and facilitating KaiC autokinase activity. At night, S431 phosphorylation in KaiC leads to changes in the flexibility of the C-terminal domain of KaiC (CII) and subsequent CII-CI ring−ring stacking (CI, N-terminal domain of KaiC).[10,11] This stacking interaction, along with ADP binding in CI enabled by CI ATPase activity,[12,13] biases KaiC toward an alternative conformation that is KaiB-binding competent[10,14] at the loop region of the N-terminal domain (B-loops).[15] This KaiB-binding competent KaiC state stabilizes a fold-switched conformer of KaiB (fs-KaiB)[16] that is capable of sequestering KaiA into a ternary KaiABC complex.[10,17] The fs-KaiB-bound KaiA adopts an autoinhibited conformation that is incapable of binding to the KaiC A-loops,[17] thus inhibiting KaiC autokinase activity and allowing the autophosphatase activity to dominate. The oscillator returns to the dawn state once hyperphosphorylated KaiC dephosphorylates and KaiA and KaiB are released from KaiABC complexes.

The KaiB-KaiC binding event is key to closing the negative feedback loop[13] to the rhythmic oscillation of the Kai system by deactivating KaiA.[17] Furthermore, KaiB provides temporal regulation of the phosphorylation levels of RpaA, the master transcription regulator,[18] through two cognate histidine kinases, SasA[19] and CikA[20] (Figure 1b). At dusk, SasA is activated on binding to $KaiC_{pSpT}$ and autophosphorylates at

Received: August 3, 2021
Published: January 3, 2022

https://doi.org/10.1021/jacs.1c08103
J. Am. Chem. Soc. 2022, 144, 184−194

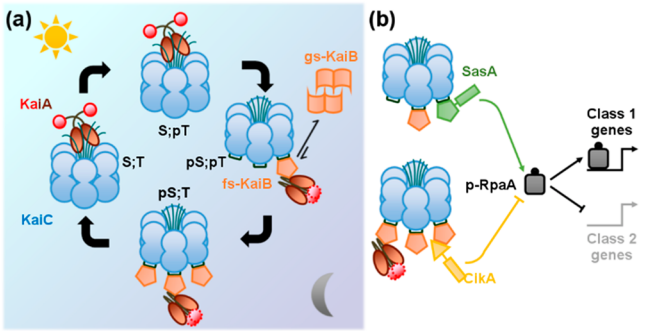

Figure 1. Model of the cyanobacterial circadian clock (Kai clock). (a) Interactions among the three core proteins, KaiA (red/brown), KaiB (orange), and KaiC (cyan) as represented by their cartoon depictions. The phosphostate of the KaiC phosphosites, serine 431 (S431) and threonine 432 (T432), cycles through the sequence S;T → S;pT → pS;pT → pS;T → S;T (p: phosphorylated). gs-KaiB and fs-KaiB represent the ground state and fold-switched state of KaiB, respectively. (b) Coupling of the core proteins with SasA (green) and CikA (yellow) to regulate RpaA phosphorylation (phosphorylated RpaA: p-RpaA), which in turn upregulates class 1 genes and downregulates class 2 genes.

SasA-H161,[21] followed by phosphotransfer to aspartyl residue 53 of RpaA and upregulation of class 1 (dusk-peaking) gene expression.[18] As the night progresses, KaiB-KaiC interactions replace that of SasA-KaiC as $KaiC_{pSpT}$ dephosphorylates to $KaiC_{pST}$, deactivating SasA. Concurrent to sequestration of KaiA, KaiC-bound KaiB recruits CikA and activates its phosphatase activity toward RpaA.[20] At dawn, KaiB-KaiC complexes dissociate on $KaiC_{pST}$ dephosphorylation to $KaiC_{ST}$, releasing KaiB-associated CikA (and KaiA) and completing an RpaA activation−deactivation cycle. On the structural level, although the N-terminal domains of SasA and KaiB share the KaiC B-loops as their binding sites,[15,16] their differential temporal associations with KaiC gate RpaA activation via (i) the faster SasA-$KaiC_{pSpT}$ versus KaiB-$KaiC_{pSpT}$ binding kinetics due to KaiB fold-switching[16] and (ii) SasA-facilitated KaiB-$KaiC_{pSpT}$ binding as a result of heterotropic cooperativity.[22] Conversely, the gating of RpaA deactivation is accomplished via cooperative CikA-KaiB-KaiC binding, with the β2 motif of fs-KaiB[17] (Figure 1b) capable of binding to either CikA or KaiA. This competition underlies the observations that CikA shortens oscillation period[16] and compensates for low levels of KaiA.[22,23] Given the pivotal role of KaiB-KaiC binding-dissociation to clock input and output, understanding the regulation of KaiB-KaiC binding at the molecular level is of prime interest to elucidating cyanobacterial circadian rhythms in general.

It has been postulated that inter-KaiB cooperativity is fundamental to regulating KaiB-KaiC binding.[17,24,25] Previous native mass spectrometry only detected $KaiC_6$, B_1C_6, and B_6C_6,[24] hinting at cooperativity while leaving open the question of existence of other stepwise B_iC_6 intermediates, i = 2, 3, 4, or 5. More recently, crystal structures of the KaiB-KaiC complex revealed that the KaiB-KaiB interface contains a salt bridge between individual KaiB protomers facilitated by R22,[17] a residue that when mutated to alanine in the *Anabaena* analogue weakened KaiB-KaiC interactions.[26] However, questions remain as to the importance of cooperativity from a kinetic standpoint as well as the strength of contributions from nearby charged residues that were not well resolved in either crystal or cryo-EM structures.[17,27] In this study, we investigate the role of cooperativity in KaiB-KaiC binding by site-directed spin labeling (SDSL) of KaiB at K25. We show that KaiB-KaiC binding is a multistep process, resulting in two spectroscopically distinct populations of KaiC-bound KaiB. One population corresponds to KaiC-bound KaiB that has an adjacent KaiB on its α1 interface ("bulk sites", B_+), whereas the other corresponds to KaiC-bound KaiB with adjacent KaiC sites unoccupied ("edge sites", B_). We demonstrate that edge sites are intermediate states capable of recruiting KaiB for cooperative KaiB-KaiC binding, thereby reducing edge and increasing bulk sites, and that antagonization of KaiB-KaiC interactions increases edge and decreases bulk sites. We further show that the bulk ⇌ edge equilibrium is tuned via KaiC phosphorylation status and KaiA. The implications of these results are discussed in the context of the full oscillator.

RESULTS

Spin Labeling Reveals Two Subpopulations of KaiC-Bound KaiB. Wild-type KaiB does not possess native cysteines and is therefore amenable to site-directed mutagenesis to cysteine followed by spin labeling. To investigate inter-KaiB cooperativity, we spin-labeled KaiB at K25, a residue that is solvent exposed in tetrameric ground-state KaiB (gs-KaiB, Figure 2a)[28] but contributes to the KaiB-KaiB interface in $KaiB_6C_6$ (Figure 2b),[17,27] to give KaiB-K25C-3IAP ($K25C_{3IAP}$ hereafter; 3IAP: 3-iodoacetamido-PROXYL). $K25C_{3IAP}$ was determined to be fully labeled by intact mass spectrometry (Figure S1), and it served as a functional surrogate of WT-KaiB for the reconstitution of the *in vitro* KaiABC oscillator and for the binding kinetics of KaiC-KaiB, as indicated by fluorescence anisotropy (Figure S2) and native-PAGE (Figure S3), respectively.

The continuous-wave electron paramagnetic resonance (cw-EPR) spectrum of $K25C_{3IAP}$ alone displayed at least two motional dynamics states and could be simulated as such (Figures 2c and S4). Both motional components possessed isotropic rotational correlation times (Table S1) faster than twice the predicted value derived from the Stokes−Einstein relation,[29,30] suggesting that the observed motions are due to local dynamics. Plausible explanations to multiple nitroxide motional components with differing mobilities at a single labeling site include intrahelical interactions[31] and diastereomeric spectroscopic resolution.[32]

$K25C_{3IAP}$ responded spectroscopically to $KaiC_{S431E,T432E}$ ($KaiC_{EE}$), a phosphomimetic that mimics the dusk state (Figure 2c), suggesting local environment perturbation around the nitroxide moiety on binding $KaiC_{EE}$. Curiously, stoichiometric $KaiC_{EE}$ (as monomer:monomer ratio) resulted in a decrease in h_0 transition intensity (~329 mT), whereas its intensity was partly restored with excess $KaiC_{EE}$ (Figure 2c). Further analysis revealed that the spectra of free $K25C_{3IAP}$, with stoichiometric or 10-fold $KaiC_{EE}$, were linearly independent (Figure S5). Such linear independence behavior was not observed when $KaiC_{EE}$ was substituted with a monomeric KaiCI construct (Figure S6)[10] or in our previous work with $N19C_{3IAP}$.[29] The formation of nonequivalent spectra upon adding differing ratios of $KaiC_{EE}$ to $K25C_{3IAP}$ implies the formation of $KaiBC_{EE}$ complexes of differing stoichiometries and the existence of substoichiometric $KaiB_iC_6$, i < 6. This conclusion is qualitatively consistent with previous native mass spectrometric results which suggested that KaiB could bind to KaiC as B_1C_6 or B_6C_6 complexes,[24] with stoichiometric $KaiC_{EE}$ favoring B_6C_6, whereas excess $KaiC_{EE}$ favoring B_1C_6 instead.

https://doi.org/10.1021/jacs.1c08103
J. Am. Chem. Soc. 2022, 144, 184−194

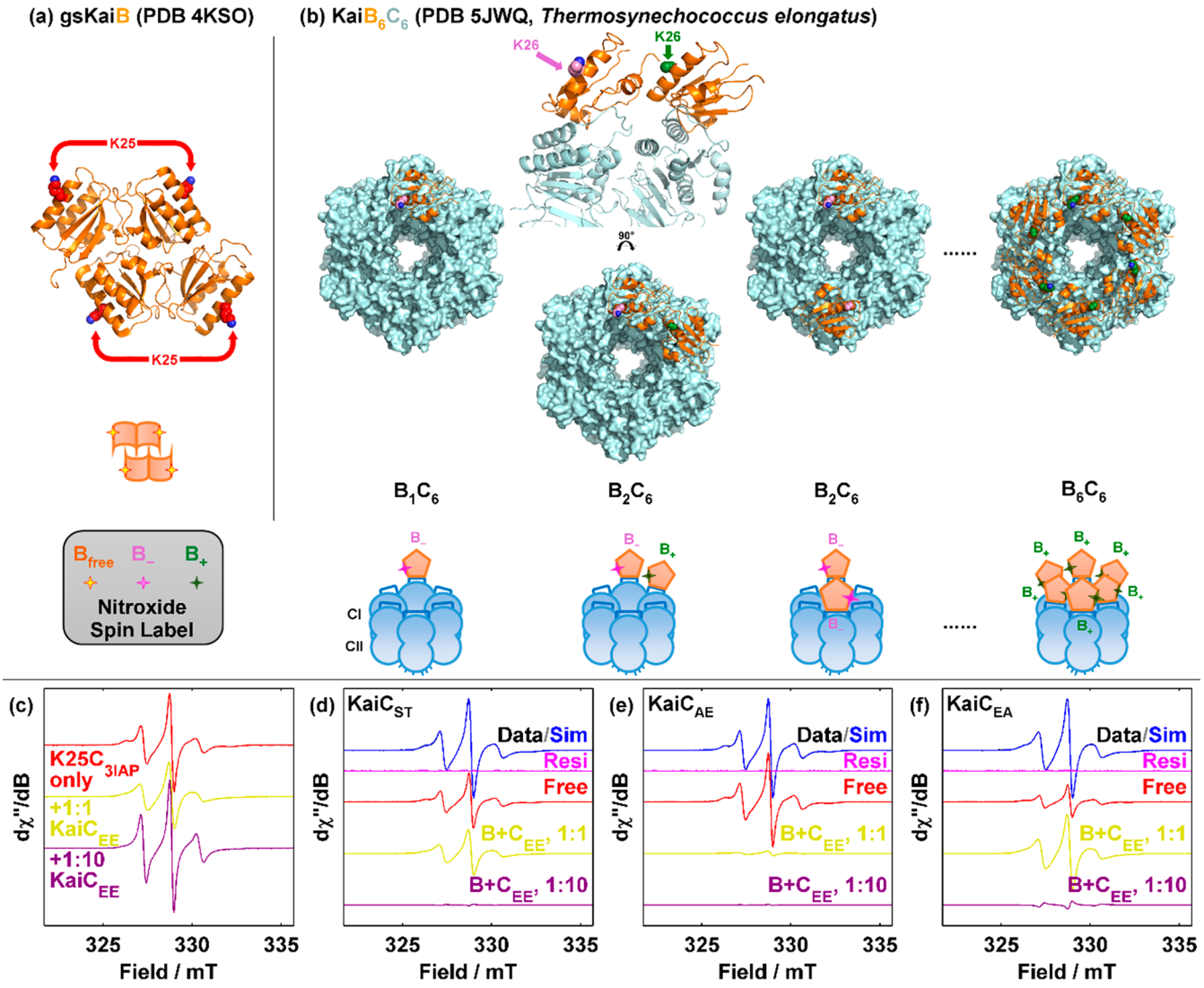

Figure 2. Site design for probing the role of cooperativity in the Kai oscillator. (a) Free KaiB (bright orange) with the side chain of labeling position $K25C_{3IAP}$ shown in red. (b) $KaiB_6C_6$ and presumed substoichiometric KaiBC intermediates prior to $KaiB_6C_6$ formation. KaiC is shown as a light blue surface. The two types of KaiBC sites, "bulk" (B_+) and "edge" (B_), are shown in green and light purple, respectively. Part of the side chain in chain B, K26 of the crystal structure of $KaiB_6C_6$, is missing. For (a) and (b), the side chain atoms of K25 (K26 in *T. elongatus*) are shown as spheres with lysyl nitrogen atoms shown in blue. Cartoon models are shown along the bottom. Bottom left box shows legend for spin labels and their corresponding spectroscopic classification. (c) Comparison of spectra of $K25C_{3IAP}$ alone (red) versus incubation with stoichiometric (dark yellow) and 10-fold excess (purple) $KaiC_{EE}$. (d–f) Reproduction of $K25C_{3IAP}$-$KaiC_{ST}$ (d), $KaiC_{AE}$ (e), and $KaiC_{EA}$ (f) reaction spectra (black) using a linear combination of free $K25C_{3IAP}$ and $K25C_{3IAP}$-$KaiC_{EE}$ spectra in (c) (blue). For (c–f), reaction spectra shown are averaged between t = 15–18 h after reaction initiation, and the residual from the fit are shown in magenta.

Furthermore, the spectra of $K25C_{3IAP}$ in the presence of stoichiometric unphosphorylated KaiC ($KaiC_{ST}$, Figure 2d), and $KaiC_{S431A,T432E}$ ($KaiC_{AE}$, Figure 2e) and $KaiC_{S431E,T432A}$ ($KaiC_{EA}$, Figure 2f), two constructs mimicking, respectively, the dominant phosphostates $KaiC_{SpT}$ and $KaiC_{pST}$ during the day and at night,[5] could all be fit by linear combinations of free KaiB, 1:1, and 1:10 KaiB:$KaiC_{EE}$ spectra. Like $N19C_{3IAP}$,[29] $K25C_{3IAP}$ did not show a cw-EPR spectral response at physiological ratios of KaiB to KaiA (Figure S7).[33,34] Combined, these results suggest that $K25C_{3IAP}$ serves as a probe for cooperative KaiB-KaiB interactions by distinguishing free KaiB from two subpopulations of KaiC-bound KaiB. These subpopulations are assigned as arising from contributions from "neighbored" (B_+) and "neighborless" (B_) fs-KaiB, analogous to bulk and edge sites found in materials (Figure 2b). Under this assignment, B_+ corresponds to fs-KaiB that is bound to KaiC and has an adjacent fs-KaiB on KaiC on the α1 interface (green pentagons in Figure 2b), whereas B_ is bound to KaiC and has no adjacent fs-KaiB on the α1 interface (light purple pentagons in Figure 2b). Thus, our EPR results suggest that there are two distinctly different KaiB populations when bound to KaiC, B_+ and B_.

Stepwise Assembly of the KaiBC Complex. A long-standing question concerns the steps involved in the assembly of the dodecameric $KaiB_6C_6$ complex starting from hexameric KaiC and tetrameric KaiB. To facilitate modeling of the binding kinetics and comparison of multiple kinetic models, we estimated the spectra of B_+ and B_ via spectral simulations (see SI text 1.1 and Figure S8–18). We focused on $KaiC_{ST}$ and KaiC phosphomimetics (Figures 3 and 4) in the absence of KaiA to preclude changes in KaiC phosphostate from contributing to any observed KaiB-KaiC binding kinetics.

https://doi.org/10.1021/jacs.1c08103
J. Am. Chem. Soc. 2022, 144, 184–194

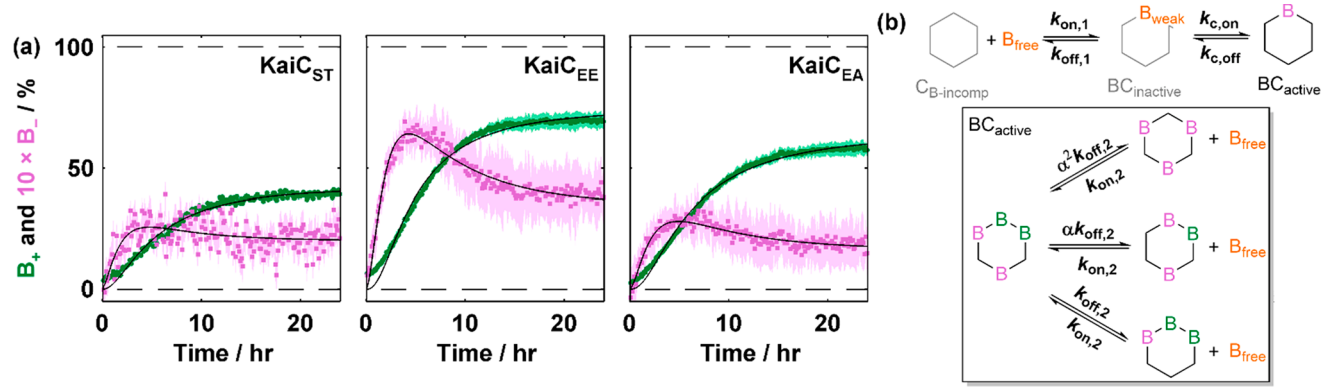

Figure 3. Stepwise assembly of KaiB-KaiC complexes as revealed by B_+ and B_ kinetics. (a) cw-EPR derived KaiB-KaiC$_{ST/EE/EA}$ kinetics using K25C$_{3IAP}$ as a probe. Black solid lines show fits to model (SI Appendix, Table S13). Green circles and light purple squares correspond to the percentages of B_+ and B_, respectively. Shaded areas: 95% CI (KaiC$_{ST}$, signal-to-noise, n = 1; KaiC$_{EE/EA}$, inter-replicate, n = 6). (b) Scheme for modeling. KaiC is assumed to adopt two conformations, inactive (gray) and active (black). Free KaiB (B$_{free}$, orange) forms an encounter complex with inactive KaiC as a weak complex (B$_{weak}$) that possesses identical cw-EPR spectrum as B$_{free}$. The encounter complex can either dissociate or change conformation to give a stably bound B_1C_6 complex in which KaiC is activated and KaiB is fold switched, giving rise to B_ (light pink). Further, KaiB binding occurs in a fashion described by Koda and Saito and give rise to B_+ (green).

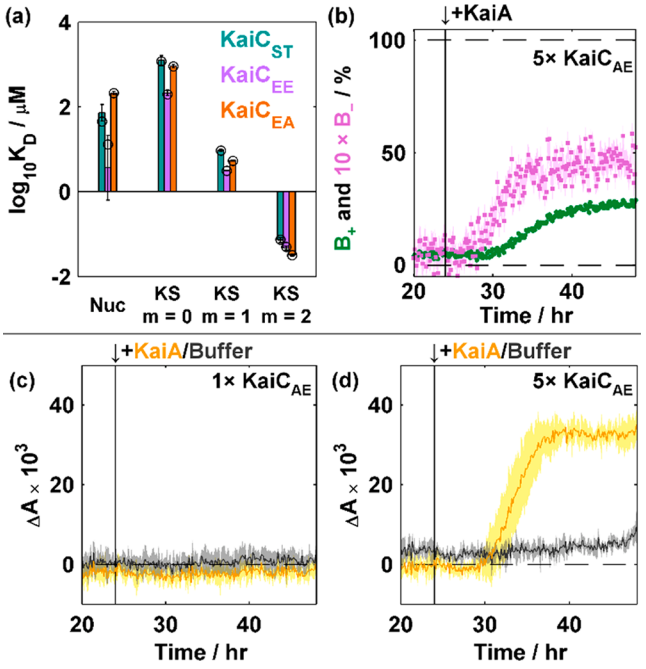

Figure 4. KaiC$_{pSpT}$, not KaiC$_{SpT}$, seeds KaiB-KaiC interactions in the day-to-night transition. (a) The effective dissociation constants for each step in KaiB-KaiC binding in the encounter complex-stepwise binding model are plotted as bar graphs for KaiC$_{ST}$ (turquoise), KaiC$_{EE}$ (purple), and KaiC$_{EA}$ (orange). Error bars show standard deviation estimated by bootstrap resampling the original data set 20 times (see Table S14). Best fit results are shown as black open circles. (b) cw-EPR-derived kinetics of KaiB-KaiC$_{AE}$ binding with KaiA spiking at t = 24 h. Green circles and light purple squares correspond to the percentages of B_+ and B_, respectively. Shaded areas: 95% CI (signal-to-noise, n = 1). (c) and (d) Fluorescence anisotropy-based KaiB-KaiC$_{AE}$ binding assays under (c) 1× and (d) 5× Kai protein concentrations with full-length KaiA (yellow) or buffer (gray) spiking at t = 24 h (black line in all panels) using 50 nM KaiB-K25C-6IAF as fluorescence probe. In both panels, basal anisotropy based on KaiB alone were subtracted. Shaded areas show inter-replicate 95% CI (n = 3).

KaiB was capable of binding to KaiC$_{ST}$, KaiC$_{EE}$, or KaiC$_{EA}$ in the absence of KaiA (Figure 3a). Here, B_+ was observed as the dominant steady-state species, whereas B_ was only present in small quantities (<10%), with the latter reaching maximum concentration at approximately t = 4 h after initiation (Figures S19 and 20). Whereas initial B_ formation could be described by a pseudo-first-order reaction, the formation of B_+ displayed sigmoidal kinetics, consistent with native PAGE data (Figure S3) as well as N19C$_{3IAP}$-KaiC$_{EE}$ binding data.[29] Furthermore, our data support the intermediacy of B_ as a precursor to B_+ as apparent from overlay plots of $d[B_+]/dt$ and [B_] showing similar time dependencies (Figure S19).

To evaluate the mechanism of KaiB-KaiC binding, we considered the model employed by Koda and Saito[35] as a starting point due to its explicit treatment of hexameric KaiC with each possessing varying amounts of KaiC-bound KaiB (Figure S21a). Briefly, this model assumes a fixed KaiB-KaiC binding rate k_{on}, but the dissociation rate $k_{off,0}$ is suppressed by adjacent KaiB subunits m (= 0, 1, or 2) in any KaiC-bound KaiB by a factor α^m. Although the sigmoidal shape of the B_+ kinetics observed in our experiments were recovered (Figure S21b,c, Table S7), their model also produced "burst-phase" behavior in B_ formation at t = 0.1 h and failed to approach steady-state by t = 15 h. To address this discrepancy, we first considered four additional models that couple with the Koda−Saito model with previously known phenomena typically associated with conformational selection, namely KaiB fold-switching,[16] KaiB tetramer-monomer equilibria,[24] and CI ATPase activity[13,14] or combinations thereof (see SI text 1.2, Figures S22−25, and Tables S8−S11). However, these models resulted in fits that overestimated the initial B_ formation in the time window t = 0−3 h.

As incorporation of previously known phenomena into the Koda−Saito model failed to explain the observed kinetics, alternative models were sought. As a first attempt, we assumed that the initial KaiB-KaiC nucleation event ($B_{free} + C_6 \rightleftharpoons B_1C_6$) possessed different rate constants from subsequent binding (Figure S26, Table S12). In effect, this nucleation event "primes" KaiC and locks KaiC into some KaiB-binding-compatible state. Curiously, this model reduced the overestimation of initial B_ formation as compared to conformational selection-based models. To expand upon this observation, we considered the formation of an encounter complex

https://doi.org/10.1021/jacs.1c08103
J. Am. Chem. Soc. 2022, 144, 184−194

between KaiB and KaiC followed by induced fitting for the nucleation event (Figure 3b, Table S13), with subsequent binding kinetics following that described by Koda and Saito.[35] In this model, KaiC initially exists in an inactive state that is unable to bind to KaiB strongly (gray in Figure 3b), presumably due to slow ATP hydrolysis in CI.[13,14] However, this inactive KaiC can form a weak encounter complex with KaiB ($BC_{inactive}$ in Figure 3b) in which the $K25C_{3IAP}$ spectral signature is identical to that of free KaiB. This weak encounter complex then establishes an equilibrium with the KaiB binding-competent state (BC_{active}, black in Figure 3b), a process in which B_ (light purple in Figure 3) is generated. This B_1C_{active} complex acts as a nucleation site to allow further KaiB-KaiC interactions in a manner described by Koda and Saito.[35] Such a model could satisfactorily reproduce the experimental KaiB-$KaiC_{ST/EE/EA}$ binding kinetics for both B_+ and B_ (Figure 3a, Table S13). Thus, apart from confirming the stepwise nature of KaiB-KaiC complex formation from C_6 to B_6C_6 via intermediates B_iC_6 (i = 2, 3, 4, or 5), our data also hint at the existence of an encounter complex, with its nature to be examined in the future (see Discussion section).

$KaiC_{pSpT}$, not $KaiC_{SpT}$, Promotes KaiB-KaiC Interactions in the Day-to-Night Transition. The day-to-night transition is characterized by KaiC S431 phosphorylation and an increase in KaiB-KaiC interactions.[36] To determine which of the KaiC phosphostate, pS;pT or pS;T, is most responsible for nucleating KaiB-KaiC interactions, we quantified the effective equilibrium constants for $KaiC_{ST/EE/EA}$ by defining either $K_{D,nuc} = \frac{k_{off,1}}{k_{on,1}} \times \frac{k_{c,off}}{k_{c,on}}$ (nucleation event in induced fit model, see derivation in text associated with Figure S27) or $K_{D,KS,m} = \frac{\alpha^m k_{off,2}}{k_{on,2}}$ (Koda−Saito steps, m = 0, 1, or 2). In all models considered, $KaiC_{EE}$ possessed the smallest initial dissociation constants $K_{D,nuc}$ and/or $K_{D,KS,m=0}$ among $KaiC_{ST}$, $KaiC_{EE}$, and $KaiC_{EA}$ (Figure 4a, Figure S27a, and Table S14).

As $KaiC_{SpT}$ precedes $KaiC_{pSpT}$ in the KaiC phosphorylation cycle,[5,6] we also investigated the potential contribution of $KaiC_{SpT}$ in seeding KaiB-KaiC interactions by reacting $K25C_{3IAP}$ with $KaiC_{AE}$. Unlike in the cases of $KaiC_{ST/EE/EA}$, $K25C_{3IAP}$ alone was incapable of binding to $KaiC_{AE}$ (Figure S28), consistent with immunoprecipitation[14] and fluorescence anisotropy results.[37] To mimic midday conditions in which $KaiC_{SpT}$ associates with KaiA, KaiA was added to the KaiB-$KaiC_{AE}$ reaction mixture. Inclusion of KaiA led to a sigmoidal increase in B_ and B_+ concentrations (Figure 4b), an observation that was paralleled by the analogous $N19C_{3IAP}$-$KaiC_{AE}$ (Figure S29a) and fluorescence experiments carried out at 5× Kai protein concentrations but not at the standard 1× concentration (1.2 μM KaiA, 3.5 μM KaiB, and 3.5 μM KaiC, Figure 4c,d, Figure S29b). The cw-EPR formation kinetics of B_ preceded that of B_+ in the ternary KaiA-KaiB-$KaiC_{AE}$ system, as revealed by the nonlinear correlation between them (Figure S28c), reinforcing the intermediate status of B_ as a bridge between free KaiB and B_+. The C-terminal domain of KaiA ($KaiA_{181-284}$, henceforth referred to as C-KaiA), a KaiA construct devoid of the KaiB-binding motif, is less effective at driving KaiB-$KaiC_{AE}$ binding (Figure S29a), hinting at the role of ternary complex formation[15,17] in stabilizing KaiB-$KaiC_{AE}$ interactions. However, parallel real-time ATPase assays[22] (Figure S29c) and fluorescence assays at reduced ATP/ADP ratios (Figure S29b) suggest that KaiA-promoted KaiC ATPase activity[7,8,38] and consequent ATP depletion at the 5× concentration contributed to the observed KaiB-$KaiC_{AE}$ interactions. Since the [ATP]/([ATP] + [ADP]) levels in cyanobacterial cultures have been estimated to fall to a minimum of 40% even in prolonged darkness,[39] this cooperative KaiA-KaiB-$KaiC_{AE}$ binding is unlikely to be the main pathway in seeding KaiB-KaiC interactions during the day-to-night transition *in vivo*. Combined, our data imply that $KaiC_{pSpT}$ is the most competent KaiC phosphostate in initializing KaiB-KaiC interactions by stabilizing KaiBC nucleation sites.

Freed KaiA Enhances Night-to-Day Transition by Promoting Dissociation of KaiB from $KaiC_{pST}$. Apart from KaiC dephosphorylation, the night-to-day transition of the Kai oscillator is also characterized by a reduction in KaiB-KaiC interactions and KaiBC-sequestered KaiA.[36] To examine the role of KaiA during the night phase, we subjected equilibrated $K25C_{3IAP}$-$KaiC_{EE/EA}$ mixtures to KaiA spiking (Figures 5a, S30, and S31). Although previous KaiA-induced transient antagonization of KaiB-$KaiC_{EE}$ interactions[29] was successfully reproduced with $K25C_{3IAP}$ (Figures 5a, S30, and S31), this antagonization was far more pronounced in analogous $KaiC_{EA}$ experiments (Figure 5b). Notably, preformed B_+ diminished over 8 h with concurrent generation of B_ (Figures 5b and S30). The correlation between the decrease in B_+ and the increase in B_ (Figure S32), suggests that B_ is a product of B_+ when KaiB-KaiC interactions are antagonized. Hence, our data establish B_ as an intermediate between free KaiB and B_+ in both reaction directions.

To dissect the molecular basis of this antagonization, we subjected pre-equilibrated $K25C_{3IAP}$-$KaiC_{EA}$ mixtures to the N- and C-terminal domains of KaiA (N-KaiA: $KaiA_{1-135}$; C- KaiA as above; Figure 5c). While N-KaiA was incapable of antagonizing KaiB-$KaiC_{EA}$ interactions, the C-terminal domain of KaiA was found to be more effective than full-length KaiA (Figure S33). As C-KaiA contains an α-helical bundle capable of binding to KaiC CII A-loops[9,40] but lacks the KaiB-binding linker in the ternary KaiABC structure,[17] the enhancement in antagonization of KaiBC interactions by C-KaiA relative to full-length KaiA suggests an allosteric mechanism involving KaiA-CII interactions, possibly through CII-CI coupled nucleotide exchange.[8] Thus, contrary to previous assumptions of inactivation through ternary KaiABC complex formation,[15] our data suggest that nonsequestered KaiA released during stochastic dephosphorylation of $KaiC_{pST}$ facilitates the night-to-day transition by interacting with the CII-A loops in night-state $KaiABC_{pST}$ complexes.

Bulk ↔ Edge Interconversion in the Core Oscillator. It has been illustrated above that the B_+ and B_ subpopulations of KaiC-bound KaiB (Figure 2b) possess different reactivities. The bulk KaiC-bound KaiB (B_+) is the preferred steady-state species formed when pS431 phosphomimetics mimicking the dusk and night states or, to a lesser extent, unphosphorylated KaiC, $KaiC_{ST}$, are present (Figure 3a). On the other hand, the edge KaiC-bound-KaiB (B_) is preferentially formed when KaiB-KaiC interactions are initiated (Figures 3a and 4b) or antagonized by KaiA (Figure 5b). To study the roles of the two populations in the Kai oscillator, we measured variations in B_+ and B_ concentrations in real time in the reconstituted oscillator (Figure 6a) and compared their rhythms against the previously known sequential KaiC phosphorylation program[5,6] (Figure 5b). The cw-EPR spectra oscillated as evidenced by the periodic variation in the central transition intensity (Figure S34). When the spectra were quantitatively interpreted (Figure

https://doi.org/10.1021/jacs.1c08103
J. Am. Chem. Soc. 2022, 144, 184−194

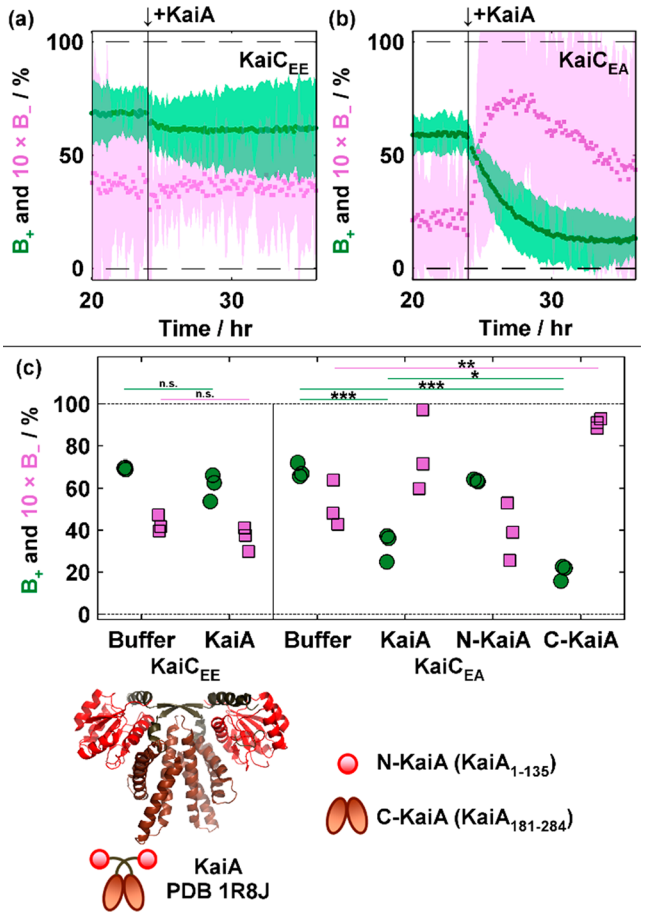

Figure 5. Nonsequestered KaiA triggers the night-to-day transition in KaiC$_{pST}$. (a) and (b) cw-EPR derived kinetics of (a) KaiB-KaiC$_{EE}$ and (b) KaiC$_{EA}$ binding with KaiA spiking at t = 24 h. Green circles and light purple squares correspond to the percentages of B$_+$ and B_, respectively. Shaded areas: 95% CI (inter-replicate, n = 3). (c) Efficacy of KaiA and its domains in antagonizing KaiB-KaiC$_{EE/EA}$ interactions. The KaiB-KaiC$_{EE/EA}$ reaction mixtures were incubated for 24 h and then spiked with buffer, full-length KaiA (KaiA), KaiA$_{1-135}$ (N-KaiA), or KaiA$_{181-284}$ (C-KaiA). Spectra were then collected within the 3.5−4 h window after spiking, and the results were binned. Top subpanel shows Tukey's HSD test (n = 3): n.s., not significant; *, $p < 0.05$; **, $p < 0.01$; ***, $p < 0.001$. Each green circle and light purple square were derived by taking the mean of spectral modeling of individual spectra. Refer to SI Appendix, Figure S30 for representative spectra. The crystal structure of full-length KaiA (PDB 1R8J) and cartoon depiction of domains tested (N-terminal domain, red; C-terminal domain, brown; linker segment, brownish-olive) are shown below.

5a), the highly reproducible dynamics (Figure S35) could be divided into an initialization phase (t = 0−12 h) and oscillation phase (t = 12−72 h, Figure S36). During initialization, sigmoidal B$_+$ binding was observed, with B_ concentration peaking at about 6 h and coinciding with the time at maximum B$_+$ rate of formation. This initialization behavior is similar to the dynamics observed in K25C$_{3IAP}$-KaiC$_{ST/EE/EA}$ binding (Figure 4a) and consistent with our model that B_ serves as a nucleation site. Once the reaction enters oscillation phase, however, B$_+$ and B_ are essentially out of phase as verified by fitting both traces to sum of cosines (Figure S37 and Table S15).

To gain further insight into the inner workings of the Kai oscillator and relate these findings to clock output, the real-time cw-EPR dynamics of KaiB were converted to phase angles to enable comparison with a previous KaiC-phosphorylation-derived model with implicit KaiB treatment by Rust et al. (Figure 6b).[5] Alignment of the phases with respect to maximal KaiB-KaiC interactions was performed under the assumption that KaiB-KaiC binding was completely described by B$_+$ and B_ (Figure 5b). Under this assumption, the interconversion of B$_+$ to B_ between ϕ = 0° to 180° occurs concurrently with KaiC$_{pST}$ dephosphorylation to KaiC$_{ST}$ and subsequent phosphorylation to KaiC$_{SpT}$. As KaiB-KaiC$_{EA}$ interactions can be antagonized by KaiA to produce B_ (Figure 5b), concurrent B$_+$ decomposition and B_ formation observed during this phase imply that KaiA is involved in promoting this phase of the clock. Our phosphomimetic data also indicated that KaiC$_{pSpT}$ promotes KaiB-KaiC interactions. pST → ST → SpT events thus ensure that sequestered KaiA can be released for the next cycle while freeing up KaiC B-loops for eventual SasA binding.[22] The buildup of B_ is facilitated by (i) a reduction in the initial $K_{D,eff}$ (m = 0) in KaiC$_{pSpT}$ relative to KaiC$_{ST}$ or KaiC$_{pST}$ (Figure S27) and to a lesser extent (ii) cooperative ternary KaiABC$_{(p)SpT}$ complex formation.[15] B_ eventually reaches a maximum at about ϕ = 180°. As demonstrated in KaiC$_{EE/EA}$ phosphomimetic experiments and kinetic modeling (Figure 4a,b), B_ is capable of recruiting B$_+$ and is responsible for the sigmoidal kinetics in those experiments. Thus, it is inferred that the buildup of B_ aids in promoting KaiB-KaiC$_{pSpT/pST}$ binding by acting as nucleation sites for further KaiB binding during the day-to-night transition between ϕ = 180° and 360°. Furthermore, KaiB-KaiC$_{EE}$ interactions are not as susceptible to KaiA-induced antagonization as is KaiC$_{EA}$ (Figure 5c). Hence, the pSpT → pST dephosphorylation event gates the clock toward the dawn state and allows sufficient time for CikA to interact with KaiC-bound KaiB.[17,22]

DISCUSSION

As KaiB-KaiC binding indirectly regulates gene expression *in vivo* via controlling the activity of two cognate histidine kinases, SasA and CikA,[20,22] that modulate the activity of RpaA, a master transcription factor (Figure 1b), the ability of the core oscillator in regulating KaiB-KaiC interactions, is of fundamental interest. We have demonstrated that differentiating the roles of "bulk" versus "edge" KaiC-bound KaiB sites is an important mechanism for regulating KaiB-KaiC interactions. The concept of differing reactivities between "bulk" and "edge" sites is a kinetic manifestation to cooperativity that has been characterized in the Kai system.[14,22] From a functional perspective, the autocatalytic nature of KaiB-KaiC binding creates a temporal delay between maximal rate of binding and maximal binding (i.e, KaiB$_6$C$_6$ ring completion). Such delay is likely to be important for ensuring a proper activation window for the output histidine kinase SasA, the latter of which preferentially binds to KaiC$_{EE}$ than KaiC$_{EA}$,[22] establishes steady-state binding to KaiC$_{EA}$ in approximately 5 h,[16] and shares a thioredoxin fold domain with fs-KaiB.[16] Unlike KaiB which exhibits edge nucleation effects, SasA displays little inter-SasA homocooperativity[25] and fails to occupy all six binding sites on the KaiC hexamer.[22] Thus, our results suggest that, in addition to fold switching between its inactive stable tetrameric fold to the active but unstable thioredoxin fold, KaiB-KaiC cooperativity provides an extra layer to regulate KaiB-KaiC binding in generating such delay.[16]

Gaps in Knowledge in How KaiB-KaiC Complexes Assemble. Our KaiB-KaiC binding data can be explained by

https://doi.org/10.1021/jacs.1c08103
J. Am. Chem. Soc. 2022, 144, 184−194

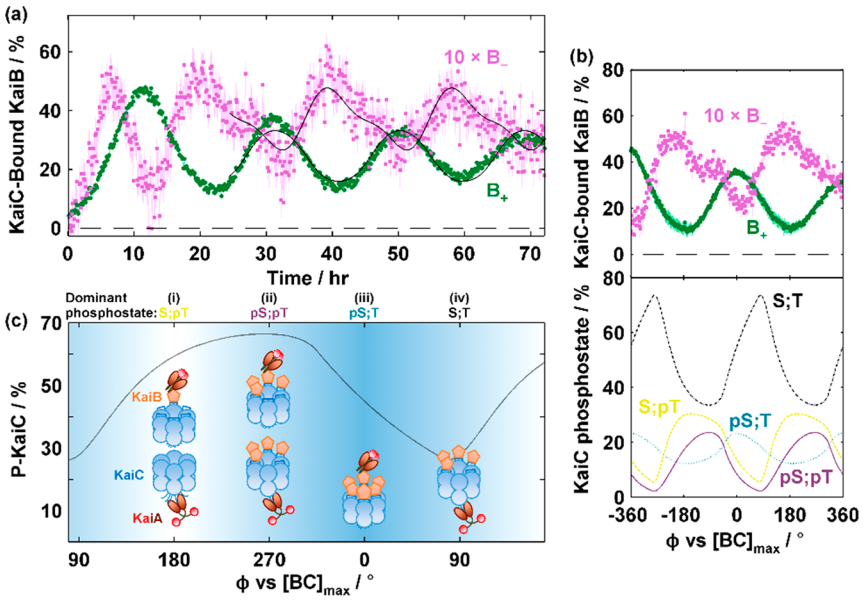

Figure 6. Dynamics of KaiC-bound KaiB subpopulations in the reconstituted Kai oscillator. (a) cw-EPR-based kinetics of B_+ and B_- as a function of time. Shaded areas represent 95% CI due to imperfect signal-to-noise. Fit to sum of cosines is overlaid as solid black lines (See SI Appendix, Table S14). (b) Stacked plot of phase relationships. The KaiC-bound KaiB populations are B_+ (green circles) and B_- (light purple squares). The KaiC phosphostates are $KaiC_{ST}$ (black dash-dot line), $KaiC_{SpT}$ (dark yellow dashed line), $KaiC_{pSpT}$ (purple solid line), and $KaiC_{pST}$ (turquoise dotted line). The SEM (n = 3) shown as shaded areas is visible at higher magnification. (c) Model of events governing KaiB-KaiC binding in the Kai oscillator. (i) During the day, KaiC (blue) is predominantly in the $KaiC_{SpT}$ state with gradual buildup in $KaiC_{pSpT}$. The former can bind to KaiB (orange) only in ATP-depleted conditions, whereas the latter can bind to KaiB unaided. This constitutes the nucleation event in KaiB-KaiC binding. (ii) As time progresses, $KaiC_{pSpT}$ builds up. Pre-existing KaiC-bound KaiB recruits further KaiB binding which provides additional fs-KaiB for sequestering KaiA (red/brown). (iii) The $KaiB_6C_6$ ring completes. With KaiA sequestered, KaiC autophosphatase activity dominates. (iv) Unlike $KaiC_{pSpT}$, KaiB-$KaiC_{pST}$ binding is sensitive to antagonization by KaiA. KaiA triggers the release of fs-KaiB from KaiC, creating nucleation sites for the next cycle.

complementing the Koda−Saito model with an encounter complex formation step (Figure 3b). Further experiments will be necessary to confirm the existence of the encounter complex and elucidate its nature. Nevertheless, our data further reinforce the notion that inter-KaiB cooperativity plays a critical role in KaiB-KaiC interactions. We point out that the induced-fit model introduced in this work is distinct from either the conformational selection model presented in our previous work, where KaiB and KaiC were assumed to establish individual equilibria to form active states prior combining to form the KaiBC complex,[16] or the two-site cooperative binding model, where KaiC was assumed to have two types of sites, with occupation of the first site by either fs-KaiB or N-SasA facilitating further KaiB-KaiC binding.[22] The necessity to use different models to explain the data may lie in the concentrations of the proteins used, with low KaiB concentrations (50 nM) obscuring intrinsic inter-KaiB cooperativity while promoting monomeric KaiB formation.[24] It is plausible that monomeric KaiB might be prone to fold-switching and could bind to KaiC without forming an encounter complex. Indeed, while the oligomeric distribution between monomeric, dimeric, and tetrameric KaiB have been estimated by native mass spectrometry,[24] the distribution between ground-state versus fold-switched KaiB has only been estimated via fitting of burst-phase KaiB-KaiC binding kinetics,[16] but not directly observed. Furthermore, conformational selection and induced fit pathways are not mutually exclusive and can depend critically on protein concentrations.[41] Despite these shortcomings in our model, the use of $K25C_{3IAP}$ in quantifying two subpopulations of KaiC-bound KaiB improves upon previous implicit treatments[5,14] and shall complement previous KaiC-phosphostate based assays.

The ability to quantify trace amounts of B_- via cw-EPR provides the first kinetic data to support inter-KaiB cooperativity. This was accomplished through detection of intermediate substoichiometric KaiBC complexes that were invisible to previous native mass spectrometry approaches.[24,25] Specifically, under all reaction conditions with typical KaiB-to-KaiC ratios considered, B_- never exceeded 10% of total KaiB. Using the augmented Koda−Saito model (Figure 3b), we estimated the fractional concentrations of strongly bound substoichiometric $KaiB_iC_6$ complexes (i = 1, 2, 3, 4, or 5) to be <10% of total KaiC (Figure S27b). Similar results were obtained when the encounter complex was neglected or when conformational selection models were assumed instead (Figure S27b). The low fractional concentrations of these substoichiometric complexes coupled with limited mass resolution in the original experiments by Snijder et al.[24] might have prevented their direct detection. These experiments should be revisited in the future as technological advances in native mass spectrometry are made.

KaiC Phosphostate-Mediated Affinity and Cooperativity Tuning. Cooperativity within KaiC hexamers was demonstrated by Lin et al.,[14] where mixtures of $KaiC_{pST}$ and $KaiC_{SpT}$ phosphomimetics were combined and assayed for their resultant KaiB binding affinities. In this study, apart from establishing the importance of inter-KaiB cooperativity in controlling KaiB-KaiC binding, we also observed phosphostate-dependent KaiB-KaiC binding in the order of $KaiC_{AE} \ll KaiC_{ST} < KaiC_{EE/EA}$. Furthermore, the presence of KaiA attenuates the relative populations of B_+ and B_-. These

https://doi.org/10.1021/jacs.1c08103
J. Am. Chem. Soc. 2022, 144, 184−194

observations imply that both KaiA and the phosphostate in CII can modulate inter-KaiB cooperativity in CI tens of angstroms away.

The computed $K_{D,eff}$ is lowest in $KaiC_{EE}$ for the nucleation step ($B_{free} + C_6 \rightarrow B_1C_6$) in all models considered (Figure S27a), suggesting that $KaiC_{pSpT}$ is more effective at KaiB-KaiC binding nucleation than $KaiC_{pST}$. This conclusion is distinct from that drawn from fluorescence anisotropy using 50 nM fluorescently labeled KaiB and variable KaiC concentrations in that the K_D between KaiB and $KaiC_{EE}$ versus $KaiC_{EA}$ were similar.[22] We speculate that this difference originates from the low concentration of KaiB used in fluorescence anisotropy experiments that might bias KaiB toward its monomeric state while precluding the observation of intrinsic inter-KaiB cooperativity, as discussed above. On the other hand, NMR spectroscopy demonstrated that KaiB-KaiC binding is enabled by an increase in CII rigidity[11] and subsequent stacking on CI,[10] which stabilizes the posthydrolysis state of CI. As T432 phosphorylation reduces CII rigidity, an explanation for the counterintuitive observation that $KaiC_{pSpT}$ has comparable or potentially higher KaiB-KaiC affinity than $KaiC_{pST}$ does (Figure 3a) is warranted but awaits more detailed studies. The $B_6C_6^{EA}$ complex has previously been crystallized,[17] whereas $B_6C_6^{EE}$ has not. Additional experiments will be necessary to determine the structural basis of these observations.

As KaiC is a member of the AAA+ ATPase family,[42] many of which are hexameric but capable of breaking their C_6 symmetry by means of differential nucleotide incorporation,[43] inter-KaiB cooperativity is likely tuned by KaiC phosphostate distribution within individual KaiC hexamers. Asymmetry in KaiC can then be introduced by intrinsic ATPase activity of CI[12] and/or nucleotide exchange in CII,[8] both of which are modulated by KaiC phosphostate.[38] Nucleotide exchange in CII has recently been modeled by molecular dynamics simulations to result in a split washer structure, with this asymmetry propagating toward CI.[8] Experimental verification of this symmetry breaking and its impact on inter-KaiB cooperativity shall be addressed in the future.

The Function of KaiA during Night-to-Day Transition and Plausible Mechanisms. Our KaiA-spiking experiments suggest that KaiA is not a passive player during the night state that is solely inactivated from promoting nucleotide exchange in KaiC.[7,8] Rather, KaiA plays an active role in antagonizing KaiB-$KaiC_{pST}$ interactions (Figure 5c). Furthermore, a reduction in KaiB-$KaiC_{pST}$ interactions implies a reduction in available fs-KaiB for sequestering KaiA in the form of ternary KaiABC complexes.[17,27] Consequently, a single KaiA dimer may trigger an autocatalytic cascade of KaiA release and further antagonization of KaiB-$KaiC_{pST}$ interactions by creating a positive feedback loop, a model to be tested. In the context of the full oscillator, this cascade is likely initiated by and enhanced during stochastic $KaiC_{pST}$ dephosphorylation to $KaiC_{ST}$ (Figure 6b), a phosphostate that is a poorer binding partner to KaiB than $KaiC_{pST}$ (Figures 3a and 4a).

The dissociation of KaiBC complexes is a possible prerequisite to providing functional output of the oscillator by regenerating CI sites for SasA binding[20] during the next cycle. As SasA and fs-KaiB compete for overlapping binding sites with CI,[15] the ability for SasA activation by binding to KaiC depends on CI availability. KaiA-induced $KaiBC_{pST}$ antagonization provides an avenue to generate open CI sites. Coupled with the delayed KaiB-$KaiC_{pSpT}$ binding kinetics (Figure 4a) as compared to N-SasA,[16] a robust SasA activation rhythm can be generated.[22]

The molecular origin of KaiA-induced $KaiBC_{pST}$ antagonization has yet to be discovered. However, our data that C-KaiA is sufficient to antagonize KaiB-KaiC interactions (Figure 5c) lend support toward an allosteric pathway involving the interactions between KaiC CII A loops and the C-terminal domain of KaiA. We thus propose an antagonization pathway where (1) KaiA interacts with CII A-loops, resulting in (2) nucleotide exchange in CI, the former of which is the direct cause of dissociation of KaiBC complexes. In the first step, KaiA is presented with two potential sites for binding to binary $KaiBC_{pST}$ complexes. While most of KaiA is sequestered by fs-KaiB, a small fraction binds to the C-terminal A-loop and tail residues of KaiC instead.[40,44] This binding occurs as a consequence of weak but nonzero intrinsic A-loop exposure in $KaiC_{pST}$ and is enhanced on stochastic S431 dephosphorylation to unphosphorylated $KaiC_{ST}$.[15] Whether KaiA-induced antagonization is more potent in $KaiC_{pST}$ or $KaiC_{ST}$ is unknown at the moment due to the inability to perform analogous antagonization experiments on $KaiC_{ST}$ without reconstituting the oscillator, but this question may be irrelevant given the mixed-phosphostate nature of KaiC hexamers in the oscillator.[14] In the second step, the KaiA-CII A-loop and tail interaction promotes nucleotide exchange in CII[7] and weakens KaiB-KaiC interactions through two mechanisms. First, KaiA-A loop interactions loosen the hexameric CII ring, which disrupts the stacking between CII and CI[11] and breaks the symmetry within KaiC.[8] Unstacking of the rings leads to withdrawal of KaiB-binding sites in KaiC, which weakens KaiB-KaiC interactions and hence inter-KaiB cooperativity. Second, the CI-CII linker has been hypothesized to behave as a nucleotide exchange factor for CI, analogous to the A-loop and tail residues to CII.[8] As stable KaiB-$KaiC_{pST}$ interactions require B-loop exposure in CI which in turn depends on CI to be in a posthydrolysis state,[17] coupled CII-CI nucleotide exchange leads to $KaiBC_{pST}$ antagonization.

Our work supports the idea that the CI and CII rings of KaiC are coupled such that KaiA-CII interactions and KaiB-CI interactions are mutually exclusive − A-loops are maximally hidden when B-loops are maximally exposed and vice versa. Thus, KaiC might have evolved to separate daytime and nighttime activities through this long-range coupling. Furthermore, our model explains the relative strengths of various KaiA constructs in antagonizing KaiB-$KaiC_{EA}$ interactions (Figure 5c) that C-KaiA > KaiA ≫ N-KaiA ∼ control. Full-length KaiA consists of N- and C-terminal domains that are joined by a linker segment.[45] In the ternary KaiABC crystal structure, a truncated KaiA construct missing the N-terminal domain was found to be in an autoinhibited state in which the KaiA-α5 helix is bound to the C-terminal helix bundle,[17] the site implicated in KaiA-CII A-loops + tail interactions.[40,46] As this helix bundle is the active site for antagonizing KaiB-KaiC interactions, simultaneous removal of KaiA-α5 and the N-terminal domain results in the C-KaiA construct (Figure 5c) that is incapable of binding to and consequently uninhibited by fs-KaiB. This results in a constitutively active KaiA construct that is more effective at antagonizing KaiB-$KaiC_{EA}$ interactions relative to full-length KaiA. On the contrary, the N-terminal pseudo-receiver domain is capable of redox state sensing[47] but otherwise unable to regulate KaiB-KaiC interactions when isolated. Instead, its paradoxical role in full-length KaiA may lie in its ability to activate the nucleotide exchange factor activity

https://doi.org/10.1021/jacs.1c08103
J. Am. Chem. Soc. 2022, 144, 184−194

of C-terminal domain of KaiA[40,46] by competing for KaiA-α5 and exposing the C-terminal helix bundle to KaiC A-loop + tail binding.

Evolutionary Adaptations in KaiA Confer Fitness in Diverse Environments. Although the loss of KaiA results in arrhythmia in *S. elongatus*[37] and consequently a loss in fitness in light−dark cycles, its absence in *Prochlorococcus marinus MED4*[48] or truncation in strains such as *Nodularis spumigena CCY9414*[49] suggests evolutionary advantages to such modifications.[50] How fitness is conferred by the loss of KaiA in *P. marinus* has recently been addressed by Chew et al.[33] − the marine environment might provide a higher regularity of cues to *P. marinus*, whereas its smaller cellular volume renders the Kai oscillator susceptible to stochastic noise. These factors result in a KaiA-less timing mechanism that behaves as an hourglass rather than a clock.[51] In vivo, *P. marinus* KaiC (ProKaiC) might be able to directly respond to cellular ATP concentrations without an external nucleotide exchange factor as evidenced by its hyper- and hypophosphorylation when *P. marinus* is subjected to constant light or darkness, respectively.[33] This is possibly achieved by ProKaiC's intrinsically higher autokinase activity compared to KaiC in *S. elongatus*.[51] Does the elevated autokinase activity imply an increased intrinsic CI nucleotide exchange rate in ProKaiC that prevents ProKaiB-ProKaiC binding even in hyperphosphorylated ProKaiC except in ATP depleted conditions during nighttime? If so, the loss of ProKaiB-ProKaiC interactions during the night-to-day transition in *P. marinus* would be entirely dictated by photosynthetic ATP influx. Analogous ProKaiB-ProKaiC experiments are necessary in understanding the diversity in clock mechanisms within cyanobacteria. On the other hand, the biofilm-forming *N. spumigena* is found in brackish water and possesses a truncated KaiA (NodKaiA)[50] that is homologous to the C-terminal $KaiA_{181-284}$ (C-KaiA) used in our experiments (Figure 5c). The lack of the N-terminal pseudoreceiver domain as well as the fs-KaiB-binding motifs likely lead to constant activation of NodKaiA as a nucleotide exchange factor for KaiC as well as weakened KaiB-KaiC interactions. Does this truncation lead to enhanced ATP sensitivity in *N. spumigena* and render it an hourglass, not unlike *P. marinus*? Further experiments will be necessary to understand the evolutionary advantages conferred by these modifications.

CONCLUSIONS

First, by spin labeling at KaiB-K25 via site-directed mutagenesis, we demonstrated the existence of B_- and B_+, two subpopulations of KaiC-bound KaiB corresponding to edge and bulk sites, respectively. The intermediacy of B_- between free KaiB and B_+ was verified by reacting $K25C_{3IAP}$ with KaiC phosphomimetics. Second, we showed that KaiBC complexes assembled via a stepwise fashion, with hyperphosphorylated $KaiC_{pSpT}$ being the most effective at initiating KaiBC complex formation. We showed that the binding kinetics could be fitted to an induced-fit model involving an encounter complex. Third, we demonstrated the role of KaiA in antagonizing KaiB-$KaiC_{pST}$ interactions and facilitating the night-to-day transition. The ability of a truncated KaiA construct to antagonize KaiB-KaiC interactions suggested long-range allosteric coupling to be a contributing mechanism. Lastly, we developed a multiobjective optimization approach to extracting kinetics from experimental cw-EPR data by coupling spectral simulations with physicality constraints. This approach extends the applicability of cw-EPR as a bioanalytical technique to interrogate biochemical systems.

ASSOCIATED CONTENT

Supporting Information

The Supporting Information is available free of charge at https://pubs.acs.org/doi/10.1021/jacs.1c08103.

Experimental details and additional characterization data (PDF)

Accession Codes

S. elongatus (PCC 7942) KaiC, UnitProt entry Q79PF4; *S. elongatus* (PCC 7942) KaiB, UnitProt entry Q79PF5; *S. elongatus* (PCC 7942) KaiA, UnitProt entry Q79PF6.

AUTHOR INFORMATION

Corresponding Authors

Andy LiWang − *School of Natural Sciences, Chemistry and Biochemistry, Health Sciences Research Institute, and Center for Cellular and Biomolecular Machines, University of California, Merced, California 95343, United States; Center for Circadian Biology, University of California, San Diego, La Jolla, California 92093, United States*; Email: aliwang@ucmerced.edu

R. David Britt − *Department of Chemistry, University of California, Davis, California 95616, United States;* orcid.org/0000-0003-0889-8436; Email: rdbritt@ucdavis.edu

Authors

Gary K. Chow − *Department of Chemistry, University of California, Davis, California 95616, United States;* Present Address: Department of Entomology and Nematology, University of California, Davis, California 95616, United States; orcid.org/0000-0001-9200-0857

Archana G. Chavan − *School of Natural Sciences, University of California, Merced, California 95343, United States;* Present Address: Genentech, San Francisco, California 94080, United States

Joel Heisler − *Chemistry and Chemical Biology, University of California, Merced, California 95343, United States;* Present Address: Genentech, San Francisco, California 94080, United States

Yong-Gang Chang − *School of Natural Sciences, University of California, Merced, California 95343, United States;* Present Address: Monash Biomedicine Discovery Institute, Monash University, Clayton, Victoria 3800, Australia

Ning Zhang − *School of Natural Sciences, University of California, Merced, California 95343, United States*

Complete contact information is available at: https://pubs.acs.org/10.1021/jacs.1c08103

Notes

The authors declare no competing financial interest.

ACKNOWLEDGMENTS

We thank Drs. William Jewell and Armann Andaya for their help in acquiring LCMS data. We thank Professors Adam Moule and Carrie L. Partch and Dr. Lu Hong for valuable insights. This work was supported by grants from the U.S. National Science Foundation (NSF-MCB-1615752 to R.D.B.; NSF-HRD-1547848 to CREST: Center for Cellular and Biomolecular Machines at UC Merced), National Institutes

of Health (GM107521 to A.L.), and Army Research Office (W911NF-17-1-0434 to A.L.).

REFERENCES

(1) Dunlap, J. C. Molecular Bases for Circadian Clocks. *Cell* **1999**, *96* (2), 271−290.
(2) Lambert, G.; Chew, J.; Rust, M. J. Costs of Clock-Environment Misalignment in Individual Cyanobacterial Cells. *Biophys. J.* **2016**, *111* (4), 883−891. Ouyang, Y.; Andersson, C. R.; Kondo, T.; Golden, S. S.; Johnson, C. H. Resonating circadian clocks enhance fitness in cyanobacteria. *Proc. Natl. Acad. Sci. U. S. A.* **1998**, *95* (15), 8660−8664.
(3) Nakajima, M.; Imai, K.; Ito, H.; Nishiwaki, T.; Murayama, Y.; Iwasaki, H.; Oyama, T.; Kondo, T. Reconstitution of circadian oscillation of cyanobacterial KaiC phosphorylation in vitro. *Science* **2005**, *308* (5720), 414−415.
(4) Tomita, J.; Nakajima, M.; Kondo, T.; Iwasaki, H. No transcription-translation feedback in circadian rhythm of KaiC phosphorylation. *Science* **2005**, *307* (5707), 251−254.
(5) Rust, M. J.; Markson, J. S.; Lane, W. S.; Fisher, D. S.; O'Shea, E. K. Ordered phosphorylation governs oscillation of a three-protein circadian clock. *Science* **2007**, *318* (5851), 809−812.
(6) Nishiwaki, T.; Satomi, Y.; Kitayama, Y.; Terauchi, K.; Kiyohara, R.; Takao, T.; Kondo, T. A sequential program of dual phosphorylation of KaiC as a basis for circadian rhythm in cyanobacteria. *EMBO J.* **2007**, *26* (17), 4029−4037.
(7) Nishiwaki-Ohkawa, T.; Kitayama, Y.; Ochiai, E.; Kondo, T. Exchange of ADP with ATP in the CII ATPase domain promotes autophosphorylation of cyanobacterial clock protein KaiC. *Proc. Natl. Acad. Sci. U. S. A.* **2014**, *111* (12), 4455−4460.
(8) Hong, L.; Vani, B. P.; Thiede, E. H.; Rust, M. J.; Dinner, A. R. Molecular dynamics simulations of nucleotide release from the circadian clock protein KaiC reveal atomic-resolution functional insights. *Proc. Natl. Acad. Sci. U. S. A.* **2018**, *115* (49), E11475−E11484.
(9) Kim, Y. I.; Dong, G.; Carruthers, C. W.; Golden, S. S.; LiWang, A. The day/night switch in KaiC, a central oscillator component of the circadian clock of cyanobacteria. *Proc. Natl. Acad. Sci. U. S. A.* **2008**, *105* (35), 12825−12830.
(10) Chang, Y. G.; Tseng, R.; Kuo, N. W.; LiWang, A. Rhythmic ring-ring stacking drives the circadian oscillator clockwise. *Proc. Natl. Acad. Sci. U. S. A.* **2012**, *109* (42), 16847−16851.
(11) Chang, Y. G.; Kuo, N. W.; Tseng, R.; LiWang, A. Flexibility of the C-terminal, or CII, ring of KaiC governs the rhythm of the circadian clock of cyanobacteria. *Proc. Natl. Acad. Sci. U. S. A.* **2011**, *108* (35), 14431−14436.
(12) Abe, J.; Hiyama, T.; Mukaiyama, A.; Son, S.; Mori, T.; Saito, S.; Osako, M.; Wolanin, J.; Yamashita, E.; Kondo, T.; et al. Atomic-scale origins of slowness in the cyanobacterial circadian clock. *Science* **2015**, *349* (6245), 312−316.
(13) Phong, C.; Markson, J. S.; Wilhoite, C. M.; Rust, M. J. Robust and tunable circadian rhythms from differentially sensitive catalytic domains. *Proc. Natl. Acad. Sci. U. S. A.* **2013**, *110* (3), 1124−1129.
(14) Lin, J.; Chew, J.; Chockanathan, U.; Rust, M. J. Mixtures of opposing phosphorylations within hexamers precisely time feedback in the cyanobacterial circadian clock. *Proc. Natl. Acad. Sci. U. S. A.* **2014**, *111* (37), E3937−E3945.
(15) Tseng, R.; Chang, Y. G.; Bravo, I.; Latham, R.; Chaudhary, A.; Kuo, N. W.; LiWang, A. Cooperative KaiA-KaiB-KaiC interactions affect KaiB/SasA competition in the circadian clock of cyanobacteria. *J. Mol. Biol.* **2014**, *426* (2), 389−402.
(16) Chang, Y. G.; Cohen, S. E.; Phong, C.; Myers, W. K.; Kim, Y. I.; Tseng, R.; Lin, J.; Zhang, L.; Boyd, J. S.; Lee, Y.; et al. A protein fold switch joins the circadian oscillator to clock output in cyanobacteria. *Science* **2015**, *349* (6245), 324−328.
(17) Tseng, R.; Goularte, N. F.; Chavan, A.; Luu, J.; Cohen, S. E.; Chang, Y. G.; Heisler, J.; Li, S.; Michael, A. K.; Tripathi, S.; et al. Structural basis of the day-night transition in a bacterial circadian clock. *Science* **2017**, *355* (6330), 1174−1180.
(18) Markson, J. S.; Piechura, J. R.; Puszynska, A. M.; O'Shea, E. K. Circadian control of global gene expression by the cyanobacterial master regulator RpaA. *Cell* **2013**, *155* (6), 1396−1408.
(19) Takai, N.; Nakajima, M.; Oyama, T.; Kito, R.; Sugita, C.; Sugita, M.; Kondo, T.; Iwasaki, H. A KaiC-associating SasA-RpaA two-component regulatory system as a major circadian timing mediator in cyanobacteria. *Proc. Natl. Acad. Sci. U. S. A.* **2006**, *103* (32), 12109−12114.
(20) Gutu, A.; O'Shea, E. K. Two antagonistic clock-regulated histidine kinases time the activation of circadian gene expression. *Mol. Cell* **2013**, *50* (2), 288−294.
(21) Valencia, S. J.; Bitou, K.; Ishii, K.; Murakami, R.; Morishita, M.; Onai, K.; Furukawa, Y.; Imada, K.; Namba, K.; Ishiura, M. Phase-dependent generation and transmission of time information by the KaiABC circadian clock oscillator through SasA-KaiC interaction in cyanobacteria. *Genes Cells* **2012**, *17* (5), 398−419.
(22) Chavan, A. G.; Swan, J. A.; Heisler, J.; Sancar, C.; Ernst, D. C.; Fang, M.; Palacios, J. G.; Spangler, R. K.; Bagshaw, C. R.; Tripathi, S.; et al. Reconstitution of an intact clock reveals mechanisms of circadian timekeeping. *Science* **2021**, *374* (6564), eabd4453.
(23) Kaur, M.; Ng, A.; Kim, P.; Diekman, C.; Kim, Y.-I. CikA Modulates the Effect of KaiA on the Period of the Circadian Oscillation in KaiC Phosphorylation. *J. Biol. Rhythms* **2019**, *34* (2), 218−223.
(24) Snijder, J.; Burnley, R. J.; Wiegard, A.; Melquiond, A. S. J.; Bonvin, A. M. J. J.; Axmann, I. M.; Heck, A. J. R. Insight into cyanobacterial circadian timing from structural details of the KaiB-KaiC interaction. *Proc. Natl. Acad. Sci. U. S. A.* **2014**, *111* (4), 1379−1384.
(25) Murakami, R.; Yunoki, Y.; Ishii, K.; Terauchi, K.; Uchiyama, S.; Yagi, H.; Kato, K. Cooperative Binding of KaiB to the KaiC Hexamer Ensures Accurate Circadian Clock Oscillation in Cyanobacteria. *Int. J. Mol. Sci.* **2019**, *20*, 4550.
(26) Garces, R. G.; Wu, N.; Gillon, W.; Pai, E. F. Anabaena circadian clock proteins KaiA and KaiB reveal a potential common binding site to their partner KaiC. *EMBO J.* **2004**, *23* (8), 1688−1698.
(27) Snijder, J.; Schuller, J.; Wiegard, A.; Lossl, P.; Schmelling, N.; Axmann, I.; Plitzko, J.; Forster, F.; Heck, A. Structures of the cyanobacterial circadian oscillator frozen in a fully assembled state. *Science* **2017**, *355* (6330), 1181−1184.
(28) Villarreal, S. A.; Pattanayek, R.; Williams, D. R.; Mori, T.; Qin, X. M.; Johnson, C. H.; Egli, M.; Stewart, P. L. CryoEM and Molecular Dynamics of the Circadian KaiB-KaiC Complex Indicates That KaiB Monomers Interact with KaiC and Block ATP Binding Clefts. *J. Mol. Biol.* **2013**, *425* (18), 3311−3324. Hitomi, K.; Oyama, T.; Han, S.; Arvai, A. S.; Getzoff, E. D. Tetrameric architecture of the circadian clock protein KaiB. A novel interface for intermolecular interactions and its impact on the circadian rhythm. *J. Biol. Chem.* **2005**, *280* (19), 19127−19135.
(29) Chow, G. K.; Chavan, A. G.; Heisler, J. C.; Chang, Y.-G.; LiWang, A.; Britt, R. D. Monitoring Protein−Protein Interactions in the Cyanobacterial Circadian Clock in Real Time via Electron Paramagnetic Resonance Spectroscopy. *Biochemistry* **2020**, *59* (26), 2387−2400.
(30) Halle, B.; Davidovic, M. Biomolecular hydration: from water dynamics to hydrodynamics. *Proc. Natl. Acad. Sci. U. S. A.* **2003**, *100* (21), 12135−12140.
(31) Guo, Z.; Cascio, D.; Hideg, K.; Hubbell, W. L. Structural determinants of nitroxide motion in spin-labeled proteins: solvent-exposed sites in helix B of T4 lysozyme. *Protein Sci.* **2008**, *17* (2), 228−239.
(32) Wong, L.T.L.; Piette, L.H.; Little, J.R.; Hsia, J.C. Stereo-specificity of murine myeloma protein-315 to enantiomeric spin labeled dinitrophenyl hapten. *Immunochemistry* **1974**, *11* (7), 377−379.
(33) Chew, J.; Leypunskiy, E.; Lin, J.; Murugan, A.; Rust, M. J. High protein copy number is required to suppress stochasticity in the cyanobacterial circadian clock. *Nat. Commun.* **2018**, *9* (1), 3004.

https://doi.org/10.1021/jacs.1c08103
J. Am. Chem. Soc. 2022, 144, 184−194

(34) Kitayama, Y.; Iwasaki, H.; Nishiwaki, T.; Kondo, T. KaiB functions as an attenuator of KaiC phosphorylation in the cyanobacterial circadian clock system. *EMBO J.* **2003**, *22* (9), 2127−2134.
(35) Koda, S. I.; Saito, S. An alternative interpretation of the slow KaiB-KaiC binding of the cyanobacterial clock proteins. *Sci. Rep.* **2020**, *10* (1), 10439.
(36) Kageyama, H.; Nishiwaki, T.; Nakajima, M.; Iwasaki, H.; Oyama, T.; Kondo, T. Cyanobacterial circadian pacemaker: Kai protein complex dynamics in the KaiC phosphorylation cycle in vitro. *Mol. Cell* **2006**, *23* (2), 161−171.
(37) Welkie, D. G.; Rubin, B. E.; Chang, Y. G.; Diamond, S.; Rifkin, S. A.; LiWang, A.; Golden, S. S. Genome-wide fitness assessment during diurnal growth reveals an expanded role of the cyanobacterial circadian clock protein KaiA. *Proc. Natl. Acad. Sci. U. S. A.* **2018**, *115* (30), E7174−E7183.
(38) Terauchi, K.; Kitayama, Y.; Nishiwaki, T.; Miwa, K.; Murayama, Y.; Oyama, T.; Kondo, T. ATPase activity of KaiC determines the basic timing for circadian clock of cyanobacteria. *Proc. Natl. Acad. Sci. U. S. A.* **2007**, *104* (41), 16377−16381.
(39) Rust, M. J.; Golden, S. S.; O'Shea, E. K. Light-driven changes in energy metabolism directly entrain the cyanobacterial circadian oscillator. *Science* **2011**, *331* (6014), 220−223.
(40) Egli, M.; Pattanayek, R.; Sheehan, J. H.; Xu, Y.; Mori, T.; Smith, J. A.; Johnson, C. H. Loop-Loop Interactions Regulate KaiA-Stimulated KaiC Phosphorylation in the Cyanobacterial KaiABC Circadian Clock. *Biochemistry* **2013**, *52* (7), 1208−1220.
(41) Hammes, G. G.; Chang, Y.-C.; Oas, T. G. Conformational selection or induced fit: A flux description of reaction mechanism. *Proc. Natl. Acad. Sci. U. S. A.* **2009**, *106* (33), 13737−13741.
(42) Wang, J. Nucleotide-dependent domain motions within rings of the RecA/AAA(+) superfamily. *J. Struct. Biol.* **2004**, *148* (3), 259−267.
(43) Sysoeva, T. A. Assessing heterogeneity in oligomeric AAA+ machines. *Cell. Mol. Life Sci.* **2017**, *74* (6), 1001−1018.
(44) Vakonakis, I.; Sun, J.; Wu, T.; Holzenburg, A.; Golden, S. S.; LiWang, A. C. NMR structure of the KaiC-interacting C-terminal domain of KaiA, a circadian clock protein: implications for KaiA-KaiC interaction. *Proc. Natl. Acad. Sci. U. S. A.* **2004**, *101* (6), 1479−1484.
(45) Ye, S.; Vakonakis, I.; Ioerger, T. R.; LiWang, A. C.; Sacchettini, J. C. Crystal structure of circadian clock protein KaiA from Synechococcus elongatus. *J. Biol. Chem.* **2004**, *279* (19), 20511−20518.
(46) Vakonakis, I.; LiWang, A. C. Structure of the C-terminal domain of the clock protein KaiA in complex with a KaiC-derived peptide: implications for KaiC regulation. *Proc. Natl. Acad. Sci. U. S. A.* **2004**, *101* (30), 10925−10930.
(47) Wood, T. L.; Bridwell-Rabb, J.; Kim, Y. I.; Gao, T.; Chang, Y. G.; LiWang, A.; Barondeau, D. P.; Golden, S. S. The KaiA protein of the cyanobacterial circadian oscillator is modulated by a redox-active cofactor. *Proc. Natl. Acad. Sci. U. S. A.* **2010**, *107* (13), 5804−5809.
(48) Holtzendorff, J.; Partensky, F.; Mella, D.; Lennon, J. F.; Hess, W. R.; Garczarek, L. Genome streamlining results in loss of robustness of the circadian clock in the marine cyanobacterium Prochlorococcus marinus PCC 9511. *J. Biol. Rhythms* **2008**, *23* (3), 187−199.
(49) Voss, B.; Bolhuis, H.; Fewer, D. P.; Kopf, M.; Möke, F.; Haas, F.; El-Shehawy, R.; Hayes, P.; Bergman, B.; Sivonen, K.; et al. Insights into the physiology and ecology of the brackish-water-adapted Cyanobacterium Nodularia spumigena CCY9414 based on a genome-transcriptome analysis. *PLoS One* **2013**, *8* (3), e60224.
(50) Axmann, I. M.; Hertel, S.; Wiegard, A.; Dörrich, A. K.; Wilde, A. Diversity of KaiC-based timing systems in marine Cyanobacteria. *Mar. Genomics* **2014**, *14*, 3−16.
(51) Axmann, I. M.; Dühring, U.; Seeliger, L.; Arnold, A.; Vanselow, J. T.; Kramer, A.; Wilde, A. Biochemical evidence for a timing mechanism in prochlorococcus. *J. Bacteriol.* **2009**, *191* (17), 5342−5347.

https://doi.org/10.1021/jacs.1c08103
J. Am. Chem. Soc. 2022, 144, 184−194